5 Induced polarization and self-potential

The induced-polarization (IP) and and self-potential (SP) methods of geophysical exploration are based on measurements, normally made at the surface of the Earth, of electric potentials that are associated with subsurface charge distributions. In the IP method, the charge distributions are induced by an application of external electrical energy. In the SP method, subsurface charge distributions are maintained by persistent, natural electrochemical processes.

Consider the hypothetical situation shown in Figure 5.1 in which electrical charges are distributed unevenly within the subsurface. Charge accumulations are portrayed schematically in the figure as positive and negative "charge centers." The charges may be volumetrically distributed or they may reside on mineral surfaces and other interfaces. In either case, the regions where charge is concentrated can be viewed as the spatially extended terminals of a kind of natural battery, or geobattery. The sketch shown in the figure greatly simplifies the realistic charge distributions that occur within actual geological formations but it is instructive for the present purpose. Electrical energy supplied from an external source, or energy that naturally arises from a persistent electrochemical process, is required to maintain the "out-of-equilibrium" charge distributions shown in Figure 5.1. Without an energy input, they would rapidly neutralize in the presence of the conductive host medium, and the geobattery would soon discharge.

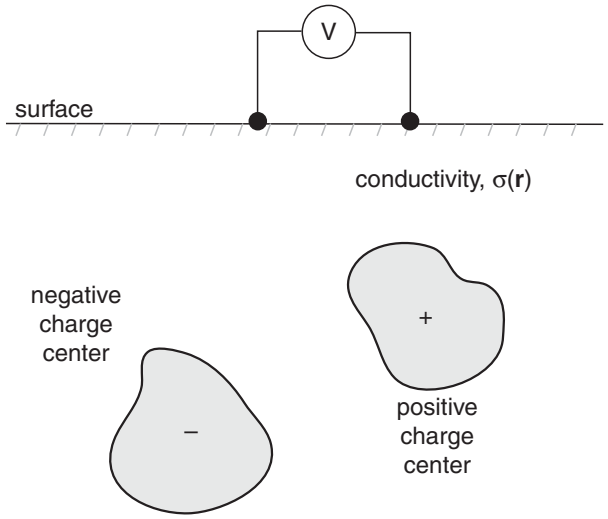

Figure 5.1 Generic subsurface charge polarization.

5.1 Induced polarization (IP): introduction

Suppose a standard resistivity experiment (see Chapter 4) is performed in which the current I is suddenly switched off at time $t = 0$. The voltage across any pair of potential electrodes normally drops instantaneously to zero. However, if the ground is *polarizable*, the voltage drops rapidly from its initial value V_0 to a non-zero value V_1 and thereafter decays slowly, often with a characteristic *stretched-exponential* shape of the form $\sim t\exp(-at^{\beta})$ with $0 < \beta < 1$, as shown in Figure 5.2. This transient behavior is known as the time-domain *IP effect*. Notice that the IP decay curve cannot be simply explained by an effective capacitance C in series with an effective resistance R in an equivalent RC circuit of the Earth. The discharge of such a capacitance after current switch off generates a transient voltage that decays purely exponentially as $\sim\exp(-t/RC)$ (Tipler, 1982), not according to a stretched exponential law.

There is not widespread agreement amongst geophysicists as to the physical explanation for the stretched-exponential shape of the transient IP decay. Significantly however, a stretched-exponential function is nothing more than a linear superposition of ordinary exponential decays. Stretched-exponential functions have been shown by many authors (e.g. Frisch and Sornette, 1997) to generally describe the macroscopic relaxation of a hierarchical or disordered system, each component of which relaxes exponentially at its own characteristic time scale. This is sometimes called the Kohlrausch–Williams–Watts relaxation law.

There are many ways to measure the time-domain IP effect in field studies and a number of different expressions have appeared in the literature. Let $V(t_0)$ be the voltage measured at some fixed time t_0 after switch-off. The *polarizability* η [mV/V] of the ground has been defined as

$$\eta = \frac{V(t_0)}{V_0}. \tag{5.1}$$

The *partial chargeability* M_{12} [ms] of the ground is its polarizability averaged over a predefined time window $[t_1, t_2]$ during the stretched exponential decay,

$$M_{12} = \frac{1}{V_0}\int_{t_1}^{t_2} V(t)dt. \tag{5.2}$$

There is a considerable amount of inconsistency throughout the geophysical literature with respect to the exact definitions of η and M_{12}. Equations (5.1) and (5.2) are commonly used, but other definitions and nomenclature have been adopted by different authors.

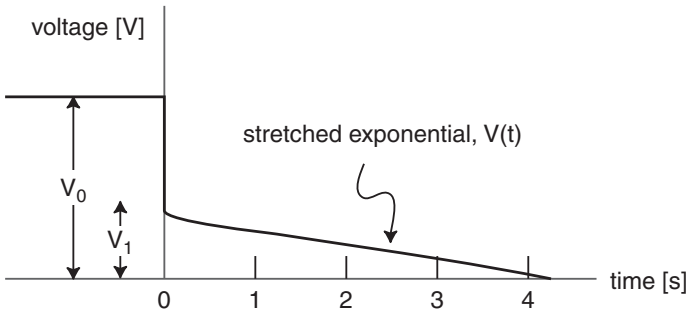

Figure 5.2 A typical IP decay curve.

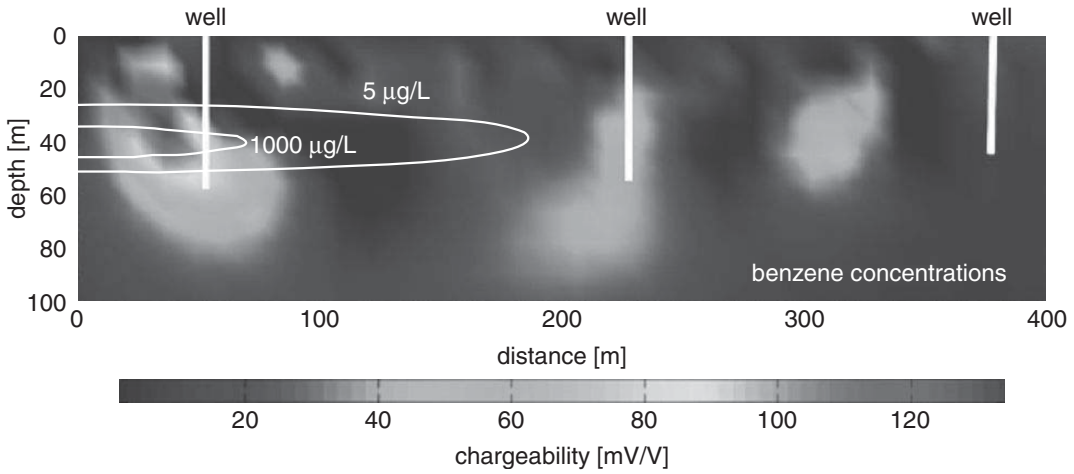

Figure 5.3 IP response of a benzene contaminant plume, Cape Cod, Massachusetts, along with contours of benzene concentration. After Sogade *et al*. (2006).

Example. IP mapping of a benzene contaminant plume.

The Massachusetts Military Reservation on Cape Cod was used as a US Air Force facility from 1948–1973. Following an uncontrolled release of jet fuel, a subsurface plume of volume 265 m^3 and length 1.5 km consisting of benzene and other organic contaminants was detected and initially characterized during the 1980s. Groundwater wells in 1996 showed benzene concentrations as high as 2500 μg/L. The geology is glacial outwash sands and gravels underlain at ~ 60 m depth by clayey lacustrine sediments. A number of laboratory-scale studies on contaminated rock and soil samples (e.g. Vanhala *et al*., 1992) have found that significant IP anomalies are associated with organic compounds such as benzene, toluene, and trichloroethene. Accordingly, time-domain IP field-scale data were acquired on-site (Sogade *et al*., 2006) in order to map the spatial extent of the plume. The two-dimensional (2-D) depth section of chargeability shown in Figure 5.3 was constructed from an IP measurement profile in the dipole–dipole configuration of total length 560 m with 24-m electrode spacing. Chargeability is defined in this study as the ratio V_1/V_0 shown in Figure 5.2, which by the definition (5.1) is essentially the polarizability η at time $t_0 = 0$. Notice that the zone of highest chargeability (~ 130 mV/V) shows a very good spatial correlation with the region of highest benzene concentration as determined by sampling of groundwater wells.

In the frequency-domain IP method, an alternating current I of frequency f, generally in the range 1 mHz–1 kHz, is injected into the ground. An IP effect is also frequently observed in the frequency domain; it appears as an out-of-phase component of electrical conduction at low frequencies (Vinegar and Waxman, 1984). Using any electrode configuration, a measure of the IP effect in the CRIU is the *percentage frequency effect PFE* defined by

$$PFE = 100\,\frac{\rho_a(f_1) - \rho_a(f_2)}{\rho_a(f_2)} \tag{5.3}$$

In Equation (5.3), $\rho_a(f_1)$ and $\rho_a(f_2)$ are the apparent resistivities measured at two frequencies f_1 and f_2 such that $f_1 < f_2$. Recall from the previous chapter that the apparent resistivity at frequency f is given by the formula

$$\rho_a = K\frac{V}{I} = KZ, \tag{5.4}$$

where K is the geometric factor of the electrode configuration and $Z = V/I$ is the impedance. In principle, any convenient electrode-array configuration can be selected for IP measurements. However, the suitability of a given array depends on a number of factors including the signal-to-noise ratio, site geology, electromagnetic-induction coupling effects at frequencies higher than ~ 100 Hz (Revil *et al*., 2012), and, as described later, electrode polarization effects. These factors are best explored by detailed forward modeling.

A second measure of the IP effect in the frequency domain is the *phase angle* ϕ [mrad] defined, at frequency f, to be the small difference in the phase of the measured voltage with respect to that of the injected current. Note that the phase of the voltage lags behind that of the causative current. In terms of the phase angle, the impedance $Z = V/I$ in Equation (5.4) has the form $Z = |Z|\exp(-i\phi)$. Inserting this expression into Equation (5.4), multiplication by the known array geometric factor K, and finally taking the reciprocal results in

$$\sigma^* = \frac{\exp(i\phi)}{K|Z|} = |\sigma|\exp(i\phi) = \sigma' + i\sigma''; \tag{5.5}$$

where σ^* is conventionally termed the *complex conductivity*. Note that the real and imaginary parts of the complex conductivity are related by

$$\sigma'' = \sigma'\tan\phi. \tag{5.6}$$

In field surveys, the complex conductivity (or equivalently, the amplitude $|\sigma|$ and phase angle φ) is measured at a single frequency. The quantity $\rho^* = 1/\sigma^*$ termed the *complex resistivity* is also frequently mentioned in the literature. The *spectral IP* (SIP) method is essentially a measurement of complex resistivity ρ^* over a range of frequencies. The SIP method is the analogous field-scale geophysical technique to AC impedance spectroscopy or dielectric spectroscopy measurements made in the laboratory on rock samples generally at higher frequencies.

5.2 Phenomenological resistivity dispersion models

A large number of empirical models have been developed to describe the frequency dependence of the electrical resistivity of polarizable geomaterials. Perhaps the simplest is the Debye model that describes a highly idealized medium relaxing according to a single exponential time decay, i.e. $V(t) = V_0 m\exp(-t/\tau)$. In the frequency domain, the Debye complex resistivity $\rho^*(\omega)$ is

$$\rho^*(\omega) = \rho_0\left[1 - m\left(1 - \frac{1}{1 + i\omega\tau}\right)\right], \tag{5.7}$$

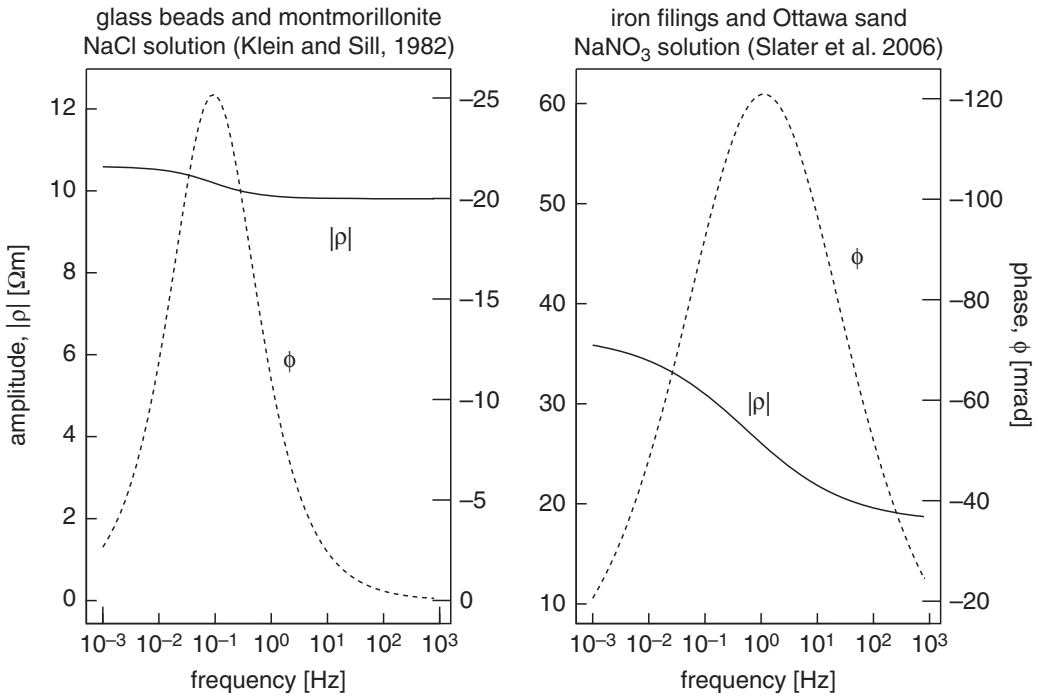

Figure 5.4 Cole–Cole complex electrical resistivity spectra.

where ρ_0 is the DC resistivity at zero frequency. The parameters m and τ [s] are termed the chargeability and relaxation time constant, respectively.

More widely used and applicable to heterogeneous geomaterials is the Cole–Cole phenomenological model (Cole and Cole, 1941; Pelton *et al*., 1978) written in the form

$$\rho^*(\omega) = \rho_0\left[1 - m\left(1 - \frac{1}{1 + (i\omega\tau_0)^c}\right)\right], \tag{5.8}$$

with frequency exponent c. The Cole–Cole model describes a material that relaxes according to a heavy-tailed distribution $g(\tau)$ of relaxation times. The distribution function $g(\tau)$ is bell-shaped and symmetric about τ_0 (Revil *et al*., 2012).

The values of the parameters m, τ_0, and c in Equation (5.8) for a given geomaterial are typically determined by a fit to experimental measurements of electrical properties made in the laboratory. For example, Klein and Sill (1982) report $m = 0.075$, $\tau_0 = 1.8$ s, $c = 0.72$ and $\rho_0 = 10.6$ Ωm for the best fit to electrical resistivity measurements over the frequency range 1 mHz–1 kHz on a mix of glass beads and montmorillonite saturated with a 0.01 mol NaCl solution. Slater *et al*. (2006b) report $m = 0.51$, $\tau_0 = 0.33$ s, $c = 0.424$ and $\rho_0 = 36.9$ Ωm for electrical resistivity measurements between 0.1 Hz–1 kHz on 10 wt.% iron filings mixed with Ottawa sand and saturated with a 0.01 mol $NaNO_3$ solution. The Cole–Cole electrical spectra using these parameters are shown in Figure 5.4. The Cole–Cole model (5.8) is phenomenological in the sense that its parameters m, τ_0, and c are not intended to be derived from basic physical arguments.

An equivalent electrical circuit (Dias, 2000) for the Cole–Cole dispersion model provides an intuitive conceptualization of the frequency-domain IP effect. The equivalent circuit is shown in Figure 5.5, where

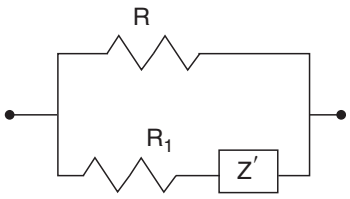

Figure 5.5 Equivalent electrical circuit for the Cole–Cole model.

$$m = \frac{R}{R + R_1}; \quad \tau = \left(\frac{R + R_1}{a}\right)^{\frac{1}{c}}; \quad Z' = \frac{a}{(i\omega)^c}; \tag{5.9}$$

and the frequency exponent obeys $0 \leq c \leq 1$. Note that the circuit contains a parallel combination of a purely resistive path R, corresponding to quasi-free ionic charge migration, and a second path of resistance R_1 and impedance Z', corresponding to charge accumulation (polarization) at subsurface interfaces. A large number of other phenomenological dispersion models, including various generalizations of the Cole–Cole function (e.g. Kruschwitz *et al*., 2010), have been proposed over the past several decades to explain IP observations. Equivalent electrical circuits for many of these models, which can become quite complex, are tabulated by Dias (2000).

5.3 Electrode, membrane, and interfacial polarization

The IP effect, measured in either the time or frequency domain, is considered by many geophysicists to be understood as follows. Suppose an electric current is caused to flow within the ground as a result of a voltage applied across a pair of current electrodes. Consider a subsurface interface, such as one between the pore-fluid electrolyte and a charged mineral surface. Such a junction is associated with contrasts in conduction mechanisms and charge-carrier mobilities, and therefore it acts as an electrochemical impedance to current flow. Charges accumulate at or near the mineral–electrolyte interface. In effect, the ground becomes polarized. In this manner, the continuous application of current from the external source forces the system into a non-equilibrium steady state in which charge distributions are built up at mineral–electrolyte interfaces. The charge distributions dissipate once the driving current is switched off.

At IP frequencies, several important mechanisms of subsurface charge accumulation, namely, *electrode polarization*, *membrane polarization*, and *interfacial polarization* have been discussed in the literature (e.g. Olhoeft, 1985). Electrode polarization is found in rocks containing mineral grains of high electrical conductivity. Metallic grains, for example, can partially block or otherwise impede the movement of ions within the pore-fluid electrolyte. The primary conduction mechanism is electronic on the metal side and ionic on the electrolyte side of a metal–electrolyte junction. Electrons are transferred across

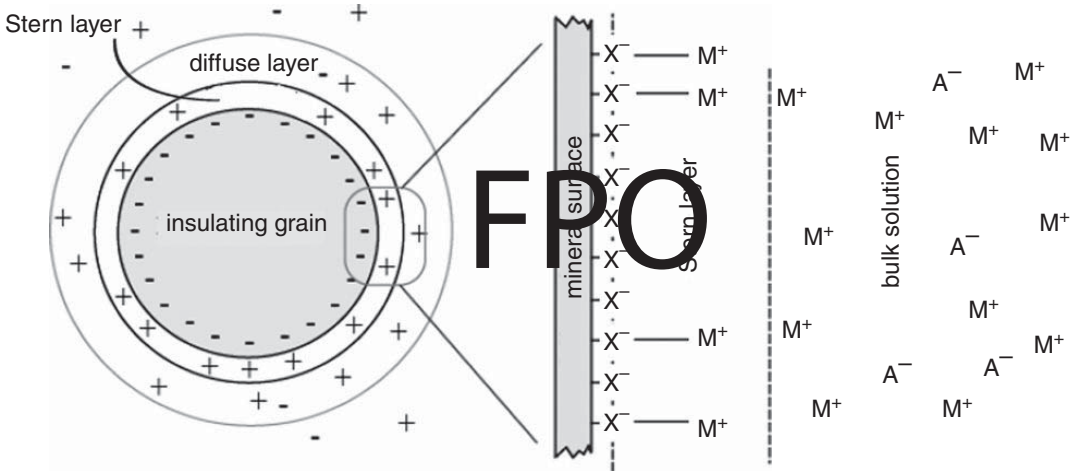

Figure 5.6 The electric double layer at the clay-mineral–electrolyte interface. After Revil and Florsch (2010).

the interface via oxidation–reduction chemical reactions. However, an energy barrier must be overcome in order for the electron transfer to proceed. It is this barrier that causes charges to accumulate at the junction, and thus an electrochemical impedance appears at metal–electrolyte interfaces.

In membrane polarization, the mobility of ions in relatively constricted pores is impeded by less-mobile ions. This can occur when electric current is passed through sediments in which clay is dispersed among larger mineral grains. Consider first the equilibrium case prior to excitation of the system by an external current. The surface of clay minerals is negatively charged. The negative surface charges attract cations from the pore-fluid electrolyte. As shown in Figure 5.6, some of these cations attach weakly to the mineral surface, contributing to the *fixed*, or *Stern layer*. Other cations form a second *diffuse*, or *Guoy–Chapman layer* within the bulk solution. The fixed and diffuse layers comprise the *electric double layer* (e.g. Parsons, 1990; Delgado *et al*., 2005) that is basic to much of electrochemistry.

Now suppose an external current is applied. The relatively poor mobility of anions and cations in the electric double layer, as shown in the figure, impedes the transport of the externally mobilized, ionic charge carriers. The magnitude of the impedance depends on the size and polarity of the charge carriers. In this manner, clay particles act as ion-selective membranes, passing some charge carriers relatively easily while preferentially impeding others. Leroy *et al*. (2008) have further suggested that the Stern layer becomes polarized when an external current is applied, without an accompanying charge buildup in the diffuse layer.

A third type of polarization, interfacial polarization or the *Maxwell–Wagner effect*, can become important at relatively high IP frequencies, greater than 1 kHz (Hizem *et al*., 2008). Interfacial polarization is a purely physical effect caused by electric charges that accumulate at conductivity interfaces within a heterogeneous medium as it is subjected to an applied electric field. We shall see in Chapter 9 that a closely related phenomenon, interfacial dielectric polarization in which charges accumulate at permittivity interfaces, can be important at the low end of ground-penetrating radar (GPR) frequencies.

5.4 IP response and subsurface geological processes

Since the IP effect originates at fluid–grain interfaces, a body that contains widely disseminated metallic or clay minerals should generate a larger IP response than a massive body containing the same total volume of metal or clay. Vinegar and Waxman (1984) report that the IP response is proportional to shaliness, a measure of the clay content, of sandstones. Slater *et al*. (2006b) have investigated in the laboratory both metal–sand and clay–sand mixtures, exhibiting electrode and membrane polarization respectively. They find that a critical parameter controlling the size of the IP effect in both cases is, indeed, the interfacial geometric factor S_p [1/μm]. As described by Pape *et al*. (1987), the factor S_p is the surface area of the mineral grains per unit volume of the saturating fluid; in other words, it is a measure of the mineral surface area that is in contact with pore electrolyte. Slater *et al*. (2006b) show that the IP response increases with the parameter S_p. The relationship $\sigma'' \sim S_p^{0.74}$ provides a good fit to data compiled from the literature by Kruschwitz *et al*. (2010), as shown by the dotted line in Figure 5.7.

A number of authors (e.g. Lesmes and Morgan, 2001; Titov *et al*., 2002) have attempted to develop first-principle theoretical models that can be used to interpret complex resistivity spectra in terms of pore microstructure and grain-size distributions, with possible implications for inferring hydraulic properties such as permeability. These models have been partially successful but this remains an area of active research. Kruschwitz *et al*. (2010), taking a phenomenological approach, suggest that small pores should lead to faster relaxation of charge polarization and hence small values of the time constant τ_0 in the Cole–Cole equation (5.8). Larger pores would lead to slower relaxation and larger values of τ_0. A number of other attempts have been made to ascribe physical meaning to the Cole–Cole parameters (e.g. Revil *et al*., 2012).

Following early studies by Olhoeft (1986) and others, there has been fast-growing interest in the application of IP field geophysical methods to characterize subsurface

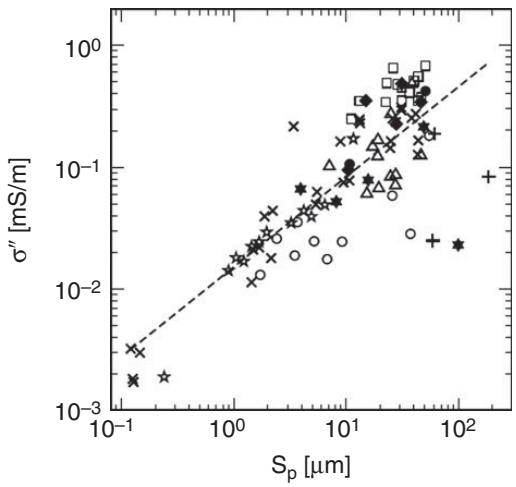

Figure 5.7 Imaginary conductivity as a function of interfacial geometric factor S_p for different geomaterials. After Kruschwitz *et al*. (2010).

organic contaminant plumes and other complex biogeochemical environments. The work of Sogade *et al*. (2006) was described earlier in this chapter. More recently, the spectral IP method was used successfully (Williams *et al*., 2009) to monitor the biostimulated subsurface activity of microorganisms that reduce metallic iron and sulfate minerals in contaminated groundwater. A primary action of the microorganisms is to convert metallic minerals into a non-metallic sulfide precipitate and hence decrease the magnitude of subsurface electrode polarization. (Doherty *et al*., 2010) used the IP method in the Wenner-array configuration (electrode spacing $a = 2.0$ m) in conjunction with self-potential, resistivity, and electromagnetic-induction geophysical data to help characterize an organic contaminant plume beneath an abandoned gasworks site in Northern Ireland. The observed chargeability anomalies were explained in terms of an electrochemical model in which ions and electrons are transferred across a thin clay layer separating perched wastewater from the underlying, biodegrading contaminant plume.

5.5 Non-polarizing electrodes

The difference in electric charge transport mechanism between the soil pore-fluid electrolyte and the metal electrodes staked into the ground results in an electrochemical impedance mismatch at the metal–electrolyte interface. If electric current passes in one direction between the soil and the electrode for an extended period of time, charge accumulates at the interface manifesting itself as an electrode polarization. The result is a spurious DC voltage. It is easy to misinterpret the spurious DC voltage as an apparent chargeability of the subsurface. The polarizability of a metal electrode depends on the type of metal employed, as shown in the study by LaBrecque and Daily (2008).

Non-polarizing electrodes reduce the electrochemical mismatch, and hence mitigate the spurious contribution to electrode polarization. Essentially, a non-polarizing electrode is one whose potential does not change upon the passage of an electric current (Bard and Faulkner, 1980). Typical materials used in the fabrication of non-polarizing electrodes are $Pb/PbCl_2$ and $Cu/CuSO_4$. The metal electrode is enclosed within a porous medium or a hard gel that is infused with a solution containing a salt of the same metal. The salt solution buffers the transition from electronic conduction in the metal electrode to ionic conduction in the soil electrolyte. The electric potential of carefully made $Pb/PbCl_2$ non-polarizing electrodes, such as those described by Petiau (2000), remains stable over time frames lasting months to years.

5.6 IP illustrated case history

Archaeological investigation of paleometallurgical activities.

The mine of Castel-Minier in France was an important source of iron, lead, and silver during the Middle Ages. Originating as a by-product of smelting, relic slag heaps contain a

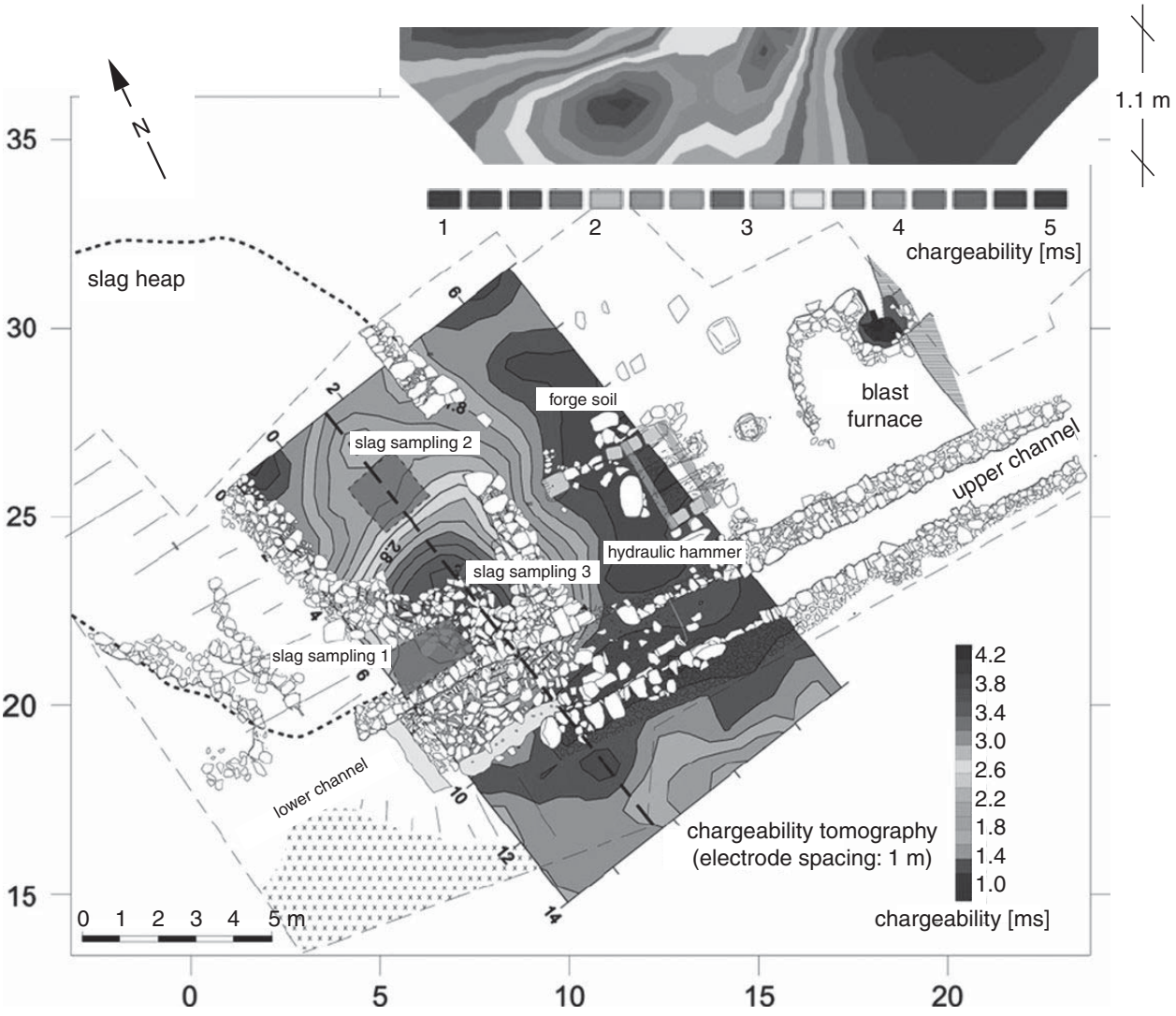

Figure 5.8 Apparent intrinsic chargeability map and vertical cross-section in support of a paleometallurgical investigation. The location of the cross-section corresponds to the dotted line on the map. After Florsch *et al.* (2010).

wealth of information of interest to metallurgical archaeologists. Of primary interest is to make a determination of the total volume of slag so that the productivity of the former mining operations can be assessed. Slag heaps contain magnetite and other metallic minerals and consequently make an excellent IP target on the basis of electrode polarization. An apparent *intrinsic chargeability* map, including a vertical cross-section, based on the IP survey conducted by Florsch *et al.* (2011) using a Wenner array (electrode spacing $a = 1.0$ m) is shown in Figure 5.8. The intrinsic chargeability m is defined in this study as the partial chargeability M_{12} between $t_1 = 10$ ms and $t_2 = 30$ ms, multiplied by $\Delta t = t_2 - t_1 = 20$ ms, so that $m = M_{12}\Delta t$. The buried slag is easily identified as the zone of high intrinsic chargeability with $m > 3$ ms. The map also shows the spatial relation of the slag heap in the larger context of the site archaeological excavation. Based on a calibration of the IP response from slag sampled from the three shaded regions in the figure, Florsch